Am J Physiol Heart Circ Physiol 295: H578–H586, 2008.
First published June 6, 2008; doi:10.1152/ajpheart.00247.2008.

Nonlinear coupling is absent in acute myocardial patients but not healthy subjects

Yan Bai,[1] Kin L. Siu,[1] Salman Ashraf,[1] Luca Faes,[2] Giandomenico Nollo,[2] and Ki H. Chon[1]

[1]*Department of Biomedical Engineering, State University of New York at Stony Brook, Stony Brook, New York; and* [2]*Dipartimento di Fisica, Universita di Trento, Trento, Italy*

Submitted 10 March 2008; accepted in final form 30 May 2008

Bai Y, Siu KL, Ashraf S, Faes L, Nollo G, Chon KH. Nonlinear coupling is absent in acute myocardial patients but not healthy subjects. *Am J Physiol Heart Circ Physiol* 295: H578–H586, 2008. First published June 6, 2008; doi:10.1152/ajpheart.00247.2008.—We investigated whether autonomic nervous system imbalance imposed by pharmacological blockades and associated with acute myocardial infarction (AMI) is manifested as modifications of the nonlinear interactions in heart rate variability signal using a statistically based bispectrum method. The statistically based bispectrum method is an ideal approach for identifying nonlinear couplings in a system and overcomes the previous limitation of determining in an ad hoc way the presence of such interactions. Using the improved bispectrum method, we found significant nonlinear interactions in healthy young subjects, which were abolished by the administration of atropine but were still present after propranolol administration. The complete decoupling of nonlinear interactions was obtained with double pharmacological blockades. Nonlinear couplings were found to be the strongest for healthy young subjects followed by degradation with old age and a complete absence of such couplings for the old age-matched AMI subjects. Our results suggest that the presence of nonlinear couplings is largely driven by the parasympathetic nervous system regulation and that the often-reported autonomic nervous system imbalance seen in AMI subjects is manifested as the absence of nonlinear interactions between the sympathetic and parasympathetic nervous regulations.

autonomic nervous system; bispectrum; heart rate variability

THE NEURAL CONTROL OF the cardiovascular system exhibits complex nonlinear behavior. One form of nonlinear behavior is the continuous interaction between the sympathetic and parasympathetic nervous activities to control the spontaneous beat-to-beat dynamics of heart rate. The interactions are believed to be nonlinear because physiological conditions would most likely involve autonomic nervous system regulation based on dynamic and simultaneous activity of the sympathetic and vagal responses to physical environmental stressors (1, 12, 26a). It is through efficient interactions between the sympathetic and parasympathetic nervous activities that the homeodynamic of the cardiovascular system is properly maintained. Failure of the interactions has been shown to lead to sympathetic hyperactivity, promoting the occurrence of life-threatening ventricular tachyarrhythmias, whereas augmented vagal tone exerts a protective and antifibrillatory effect (10, 26a). Experimental evidence suggests that hypertension (6), myocardial ischemia, acute myocardial infarction (AMI), sudden cardiac death, and chronic heart failure all exhibit signs of autonomic function imbalance (10). Consistent with autonomic imbalance, patients who have suffered an AMI have a marked decrease in heart rate variability (HRV), as demonstrated by an increase in sympathetic and a decrease in vagal neural activities. Thus, due to the condition of autonomic imbalance, it is possible that nonlinear interactions are a less common phenomenon in diseased states.

The existence of nonlinear dynamics underlying HRV in humans has been proved by a number of previous studies (3–4, 21). However, the methodological approaches proposed in these studies do not allow a physiological interpretation of the nature of the detected nonlinearities. Nonlinear heart rate dynamics may be due to the activity of several nonlinear physiological mechanisms, such as nonlinear interactions between sympathetic and parasympathetic nervous systems, but also respiratory modulations, the saturation of receptors, and others. Recently, we found evidence of the frequency modulation of the parasympathetic nervous system by the sympathetic nervous system (29) using a wavelet analysis on healthy subjects. The questions at issue are whether nonlinear HRV dynamics seen in healthy conditions can be due to nonlinear interactions between sympathetic and parasympathetic nervous systems and whether these interactions are modified with age and diseased states such as the AMI.

To address the above questions, we employed a statistical bispectrum approach, which we have recently developed to identify nonlinear interactions in the form of a quadratic phase coupling (QPC) between two components of a process (25). The definition of QPC is a condition in which a third frequency and its phase are the sum of the first two frequencies and phases. Thus QPC implies both frequency and phase coupling. Because of the properties of the bispectrum, only the phase-coupled components appear in the bispectrum. However, due to technical considerations such as using an insufficient number of segments to compute the bispectrum, frequency-coupled peaks will often appear in the bispectrum. Moreover, noise can introduce erroneous peaks. Recently, we have developed a method that overcomes these limitations of the bispectrum (25). The method is a combination of bispectrum estimation followed by testing the significance of the results against surrogate data realizations. The surrogate data transformation destroys nonlinear coupling; thus no legitimate QPC should be detected. However, any erroneous peaks will remain. The bispectrum of the surrogates, as well as the original data, is calculated. If the bispectral peaks of the original data are greater than those of the surrogate data, then they are considered to be statistically significant coupling peaks because the erroneous peaks are also exhibited in the bispectrum of the

Address for reprint requests and other correspondence: K. H. Chon, Dept. of Biomedical Engineering, SUNY at Stony Brook, HSC T18, Rm. 030, Stony Brook, NY 11794-8181 (e-mail: ki.chon@sunysb.edu).

The costs of publication of this article were defrayed in part by the payment of page charges. The article must therefore be hereby marked "*advertisement*" in accordance with 18 U.S.C. Section 1734 solely to indicate this fact.

surrogate data. Furthermore, the new approach provides an accurate and practical assessment of the coupling strength (25).

With the advent of a new statistical approach to detect nonlinear interactions, the goals of the present study were *1*) to detect nonlinear interactions in the form of QPC between the sympathetic and parasympathetic nervous activities in healthy subjects from electrocardiogram recordings, and validate the results using pharmacological interventions that block one or both branches of the autonomic nervous system, *2*) to investigate whether nonlinear interactions seen in normal subjects change with progressive aging and a cardiovascular disease state such as AMI, and *3*) to assess the role of sympathetic and parasympathetic nervous activities in the generation of nonlinear heart rate dynamics, through the statistical quantification of nervous system coupling strengths in healthy young and old subjects and AMI subjects.

METHODS

Autonomic Nervous System Blockade Protocol

The data are from a previously published study (29); thus they will be only briefly summarized. Thirty-eight volunteers (20 men and 18 women; mean age, 28 ± 6 years) were recruited. Subjects were randomly divided into two groups for experiments. Electrocardiograms sampled at 500 Hz were recorded using a Hewlett Packard Monitor (Model 78354A).

Group A. Subjects in *group A* were in supine position and underwent parasympathetic blockade, followed by complete blockade. The subjects ($n = 16$) were lying on a hospital bed during the experiment, and data were continuously recorded during control state and the administration of autonomic blockades. After baseline recordings were taken for 20 min (control state), atropine was injected (initially 0.0075 $mg \cdot kg^{-1} \cdot min^{-1}$ for 2 min followed by 0.001 $mg \cdot kg^{-1} \cdot min^{-1}$ for 23 min) to block parasympathetic nervous regulation. Data were continuously recorded the whole time. After 5 min (to allow for physiological equilibration and to prevent transient nonstationarity in each condition), propranolol was injected (initially 2 mg/min for 2 min followed by 1 mg/min for 23 min) to block sympathetic nervous regulation, resulting in the complete blockade of the ANS.

Group B. Subjects in *group B* were in upright position and underwent sympathetic blockade, followed by complete blockade. The subjects ($n = 22$) were standing comfortably in the upright position. Instead of atropine, propranolol was injected first followed by atropine. Propranolol is a known blocker of sympathetic activity. The duration of data collection and drug dosages were identical to those of *group A*.

The doses chosen for sympathetic and parasympathetic blockade with propranolol and atropine, respectively, were selected to be sufficient for the complete blockade of the parasympathetic or sympathetic system (9).

Myocardial Infarction Protocol

The data are also from a previously published study (18). The data consist of 35 post-AMI patients (age, 58.5 ± 10.2) examined 10 ± 3 days after AMI. Eight out of 35 post-AMI patients were initially under β-blocker therapy, but they discontinued treatment two half-lives before the recording session. An age-matched control group of 12 healthy subjects (63.1 ± 8.3), termed the old control, were also examined. Post-AMI patients were part of a large database collected for a Gruppo Italiano per lo Studio della Sopravvivenza nell'Infarcto Miocardio (GISSI-3) arrhythmia substudy from February 1992 to July 1993. Control subjects were normotensive and free from any known disease based on anamnesis and physical examination at the time of the study.

After a period of 15 min for subject stabilization, electrocardiograms were recorded for 10 min in the supine rest position, followed by 10 min of passive head-up tilt at 60°. All ECG signals were digitized with a 1-KHz sampling rate.

Algorithm

ECG processing. For all ECG signals, QRS complexes were detected followed by resampling to 4 Hz with a cubic spline interpolation to obtain instantaneous heart rate data. An R-R interval time series was not used since the Fourier transform used in the calculation of the bispectrum requires equally sampled data; thus we used instantaneous heart rate data instead. Subsequently, the interpolated data were detrended with second-order polynomials. Each heart rate time series contained 1,200 data points.

Meaning of frequency and phase coupling for a second-order nonlinear system. The presence of either frequency or phase coupling indicates that the system is nonlinear, and the presence of phase coupling provides additional information about the time nature of the system. The QPC or frequency coupling can be seen by passing the signal

$$x(t) = A_1 \cos(2\pi f_1 t + \phi_1) + A_2 \cos(2\pi f_2 t + \phi_2) \quad (1)$$

with A_1 and A_2 constants, through the following quadratic zero-memory nonlinear system

$$y(t) = ax(t) + bx^2(t) \quad (2)$$

in which a and b are also constants. The output of the quadratic system $\{y(t) = ax(t) + bx^2(t)\}$ contains cosinusoidal terms with the following frequencies and phases: (f_1, ϕ_1), (f_2, ϕ_2), $(2f_1, 2\phi_1)$, $(2f_2, 2\phi_2)$, $(f_1 + f_2, \phi_1 + \phi_2)$, and $(f_1 - f_2, \phi_1 - \phi_2)$. Such a phenomenon, which gives rise to the sum or difference of phases with the same relationship to that of the frequencies, is called phase and frequency coupling. If only one sinusoidal term, (f_1, ϕ_1) is passed through the quadratic nonlinear system, only the component $(2f_1, 2\phi_1)$ will result at the output. This case exhibits only self-phase and self-frequency coupling.

Surrogate data threshold method applied to the bispectrum. The direct method of calculating the bispectrum of a signal is to take the average of triple products of the Fourier transform over K segments:

$$\mathrm{BS}(f_1, f_2) = \frac{1}{K} \sum_{k=1}^{K} X_k(f_1) X_k(f_2) X_k^*(f_1 + f_2) \quad (3)$$

where X_k (f) is the Fourier transform of the kth segment and the asterisk (*) indicates the complex conjugate. Note that as the size of each segment decreases, the frequency resolution will also decrease. Therefore, it is important to choose a proper segment size so that there is sufficient resolution to resolve the dynamics in the signal while retaining enough segments to properly reduce variance in the bispectrum for the detection of QPC. As shown in *Eqs. 1* and *2*, a system with only two frequencies can lead to many different peaks in the bispectrum. However, by the design of the bispectrum, only the phase-coupled frequencies will appear, provided that a sufficiently large K in *Eq. 3* is used. An insufficient K can lead to the generation of self-coupled peaks (17). In other words, frequency-coupled and not phase-coupled signals can appear in the bispectrum if an insufficient K is used. This condition can be prevented by using as many segments as possible without compromising the ability to resolve the frequencies of interest.

In certain cases, we may not have sufficient data to have a large K, or noise-contaminated data can lead to erroneous peaks; thus we use the surrogate data technique to overcome these limitations. In addition, the surrogate data technique avoids an arbitrary selection of what is perceived to be coherent, as it is statistically based. The method involves generating 100 realizations of surrogate data from the orig-

inal data (HRV signal in this study) and calculating the bispectrum of all surrogates and the original data. Since surrogate data eliminate nonlinear components in the original data, the bispectrum of surrogate data only contain linear components. We chose the iteratively refined surrogate data technique (24) since it has been shown to be more accurate than the amplitude-adjusted Fourier transform method (27) because it iteratively corrects for deviations in the spectrum as well as maintains the correct distribution of the signal. The mean and standard deviation of all 100 surrogate bispectral estimates are calculated. The 95% statistical threshold of the surrogate data bispectrum is defined as the mean plus two standard deviations, since this assumption was verified using the Kolmogorov-Smirnov goodness of fit test (28). Any bispectral peaks estimated from the original data that are above this threshold value at each frequency are considered to have significant phase coupling. Difference values above zero will indicate a bispectral value of the original data above the threshold and are, therefore, considered significant. Since we quantify the statistical significance of the bispectral peaks via the use of a surrogate data technique, there is no need to use the bicoherence index, which has been the most widely used means to quantify the degree of nonlinear coupling. We have recently shown that the calculation of the bispectrum followed by the verification of the surrogate data provides more accurate quantification and detection of QPC (25).

Data Analysis

In both experimental protocols, stationary and artifact-free HRV signals lasting 5 min (corresponding to a variability series of 300 points, after a downsampling of HRV data to 1 Hz) were selected for each condition. For each HRV series, $K = 5$ segments (zero padding included), each containing 64 data points, with no overlapping segments, were used to estimate the bispectrum.

Only the peaks of the bispectrum that resulted above the statistical threshold values obtained via the surrogate data technique were considered for the statistical analysis. For each peak, the coupling was calculated as the difference between the bispectrum peak magnitude and the corresponding surrogate data-derived threshold value. Coupling values were presented with means ± SD of the coupling over the considered group. Differences among groups were compared with one-way ANOVA and a post hoc test. A P value of <0.05 was considered significant.

RESULTS

Examples of Application of the Algorithm

To illustrate the phase-coupling phenomenon as well as the benefit of the use of a surrogate data approach, a simple simulation example consisting of the following three frequencies is generated

$$x(t) = \sin(2\pi f_1 t + \theta_1) + \sin(2\pi f_2 t + \theta_2) + A\sin(2\pi f_3 t + \theta_3) \quad (4)$$

where f_1 and f_2 are set to 0.1 and 0.25 Hz, respectively. The third frequency, f_3, is set to $f_1 + f_2 = 0.35$ Hz to achieve the frequency coupling. Phases associated with the first two frequencies (θ_1 and θ_2) are randomly generated between $-\pi$ and π with a uniform distribution and are phase coupled such that $\theta_3 = \theta_1$ and θ_2. To the output signal x(t) we add Gaussian white noise to achieve a signal-to-noise ratio of 0 dB.

The resulting bispectra without and with the surrogate data technique are shown in Fig. 1, *A* and *B*, respectively. The power spectrum (not shown) contains only the three dominant frequencies, and because it is a linear method, it is not able to provide information regarding nonlinear phase coupling. The bispectrum, however, because it is a nonlinear method, will show only the phase-coupled component at (0.1, 0.25) Hz. However, since *Eq. 4* was contaminated with a significant additive noise source, we expect to obtain other pseudo nonphase coupled peaks, as shown in Fig. 1*A*. With the use of the surrogate technique as detailed in METHODS, only the phase-coupled peak at (0.1, 0.25) Hz appears in Fig. 1*B*. Note that the bispectral plot is symmetrical along the diagonal axis, and thus only half is shown for this and all subsequent plots.

To demonstrate the method's efficacy in quantifying the amount of phase coupling, we varied the amount of phase coupling by injecting a number of data points that had uncoupled phases. The amount of phase coupling varied from 0% to 100% at an increment of 1%. For each level of phase coupling, 100 realizations of the test signals were generated. Each realization of the test signal was corrupted by 0 dB additive Gaussian white noise. For sensitivity testing, the calculated value for each method was recorded at the known phase-coupled frequency. For specificity, the total number of significant detected peaks in the entire bispectrum was recorded, and the median between the realizations was reported. These values are shown in Fig. 1*C* as a function of the varying percent of phase coupling.

As shown in Fig. 1*C*, the percent of coupling that the method was sensitive to (Fig. 1*C*, *bottom*) was ~18%. Furthermore, it should be noted that the calculated value for the method linearly increases (Fig. 1*C*, *top*) with increasing coupling percent for values above 18%, thereby suggesting that the method provides a good quantification of the actual amount of phase coupling present in the system.

Figure 1, *D* and *E*, illustrates the benefit of using the bispectrum with the surrogate data approach for a representative healthy individual's heart rate data in the supine position as the numerous observed phase-coupled peaks in Fig. 1*D* disappear with the combined use of the bispectrum followed by the surrogate data. The peak at (0.39, 0.08) Hz signifies a phase coupling between these two frequencies or interactions between either the sympathetic and parasympathetic or parasympathetic and parasympathetic nervous activities. Note that the low frequency (LF) range of 0.04–0.15 Hz has been attributed to the actions of both sympathetic and parasympathetic nervous activities, whereas the higher frequency (HF) range of 0.15–0.5 Hz is solely due to the parasympathetic nervous activities (26a). The large peak at the LF and LF range of (0.14, 0.08) Hz as well as at the HF and HF range of (0.36, 0.25) Hz represents self coupling. Thus coupling at LF and LF could represent one of three possible scenarios: sympathetic and parasympathetic interactions, parasympathetic self coupling, or sympathetic self coupling. A peak at HF and HF represents a self coupling of the parasympathetic nervous activities.

Fig. 1. Comparison of bispectrum without (*A*) and with (*B*) surrogate data method and (*C*) illustrating specificity (*top*) and sensitivity (*bottom*) of the method in quantifying the degree of phase coupling present using a simulation example. *D* and *E*: results from a representative healthy young subject, similarly demonstrating the benefit of using the surrogate data approach. BWS, bispectrum with surrogate.

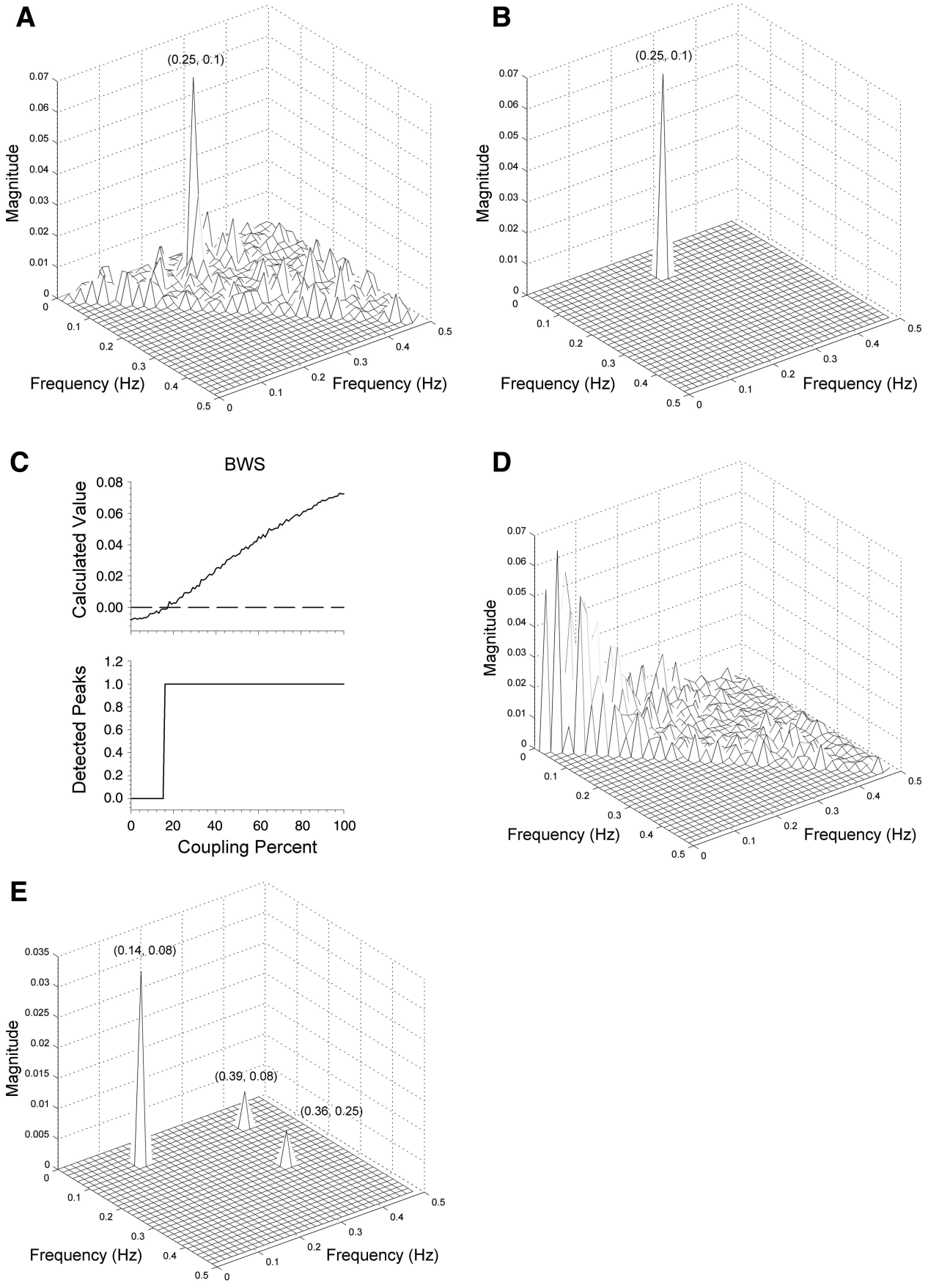

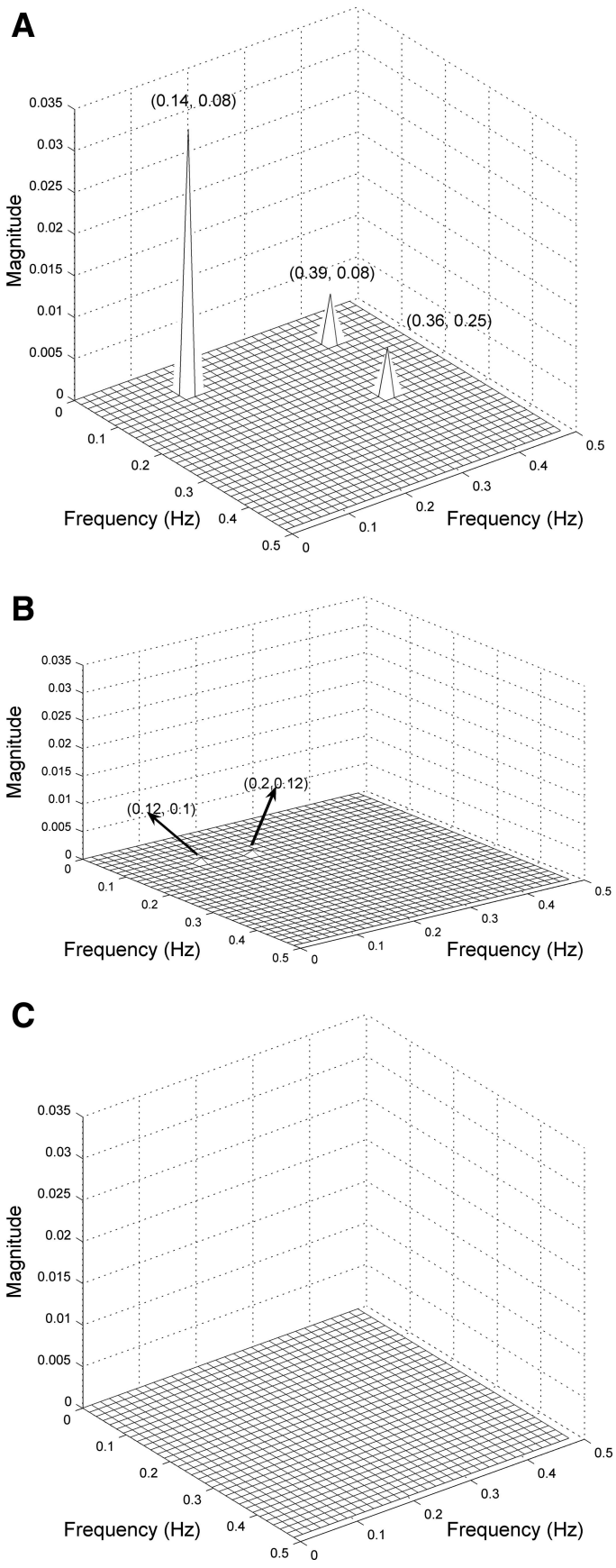

Fig. 2. Representative bispectrum results from a subject (*A*) in control condition, after administration of atropine (*B*), and after double blockades (*C*). The presence of significant phase-coupled peaks in *A* diminishes with application of atropine and completely disappears with double blockades.

Table 1. *Group average of bispectrum results indicating the presence of phase coupling pre- and postapplication of pharmacological blockades during the supine position*

Supine	LF-LF	LF-HF	HF-HF
Control	0.062±0.091	0.044±0.063	0.012±0.015
Atropine	0.00016±0.00043*	0.00048±0.00079*	0.00029±0.00061*
Double blockade	NA	NA	NA

Values are means ± SD; $n = 16$ control subjects. *$P < 0.05$, significant difference between control and atropine administration condition. LF, low frequency; HF, high frequency; NA, not applicable.

Autonomic Nervous System Blockade

Representative results from a healthy subject during supine position followed by the administration of atropine and then with double blockade (both atropine and propranolol) are shown in Fig. 2, *A–C*, respectively. The significant phase coupling between LF-LF, LF-HF, and HF-HF seen in the control state is significantly diminished with atropine, and no phase-coupled peaks are present with double blockades.

Tables 1 and 2 summarize results from subjects in the supine and upright positions, respectively, pre- and postadministration of pharmacological blockades. It should be noted that the values reported in Tables 1–4 reflect only those who had the presence of QPC, but they are the majority rather than minority among the population pool in each category. The nonapplicable values in these tables are because fewer than 50% of the subjects had detection of QPC, and for those minorities who had interactions, the values were essentially zero. During prepharmacological blockades, there are significant nonlinear interactions between LF-HF and HF-HF for both positions with additional LF-LF coupling present in the supine position. When compared with supine subjects, upright subjects show a reduced amount of interactions, since the LF-LF coupling is absent, whereas LF-HF and HF-HF coupling appear with lower magnitude (see Table 1 vs. Table 2). After atropine administration, all of the couplings are substantially abolished, as documented by the statistically significant decrease of coupling with respect to the control condition. On the contrary, the decrease of coupling observed after the administration of propranolol was slight and not statistically significant. With double blockade, nonlinear interactions are completely abolished in both body positions.

Comparison of Healthy Young, Old, and AMI Subjects

Representative bispectrum results from a young subject, an old control subject, and an AMI patient in the supine position are shown in Fig. 3. Note that the significant phase-coupled peaks in the healthy young subject become smaller with the old healthy subject. For the AMI subject, the phase-coupled peak is essentially negligible.

Tables 3 and 4 summarize the group comparison of bispectral estimates obtained from all young, old, and AMI subjects for the supine and upright positions, respectively. The young

Table 2. *Group average of bispectrum results indicating the presence of phase coupling pre- and postapplication of pharmacological blockades during the upright position*

Upright	LF-HF	HF-HF
Control	0.026±0.031	0.0066±0.016
Propranolol	0.019±0.045	0.0021±0.0026
Double blockade	NA	NA

Values are means ± SD; $n = 22$ control subjects.

subjects are the same control group as shown in Tables 1 and 2. There is no LF-LF coupling in both the old control group and the AMI group in either body position, whereas such coupling exists for the young subjects (see Table 1). In the supine position (Table 3), there is a decreasing trend in magnitudes of both the LF-HF and HF-HF coupling from the young to old control. Moreover, for the AMI patients, the coupling is essentially negligible; particularly, the HF-HF coupling is significantly lower than that of young and old control groups. In the upright position (Table 4), both the LF-HF and HF-HF couplings in AMI subjects are essentially nonexistent compared with those of the young and old control groups (the difference was statistically significant for the LF-HF coupling), whereas there was no significant difference in LF-HF and HF-HF coupling between the young and old control subjects.

DISCUSSION

In this study, we applied a novel method of surrogate data-based bispectral analysis to HRV signals to detect nonlinear interactions between the sympathetic and parasympathetic nervous activities in humans. We observed that nonlinear phase couplings exist between LF and HF oscillations of HRV and showed how these couplings are modified by the pharmacological blockade of the two branches of the autonomic nervous system and the AMI. The main findings of the study are that *1*) nonlinear interactions between the sympathetic and parasympathetic nervous activities are found in both young and old subjects; *2*) significant nonlinear coupling seen in the control cases was essentially eliminated with the sole application of atropine, and to a lesser extent with only propranolol, whereas the application of both atropine and propranolol completely abolished nonlinear interactions between the two nervous activities; and *3*) an absence of nonlinear interactions in both basal conditions and in conditions of enhanced sympathetic tone due to tilt maneuver was observed for the AMI subjects.

In our study, we found nonlinear coupling between the following frequency ranges: LF-LF, HF-HF, and LF-HF. It is well established that the LF range (0.04–0.15 Hz) represents the actions of both sympathetic and parasympathetic nervous systems (7), whereas the HF is predominantly due to the activation of the parasympathetic nervous system (26a). A recent study has suggested that increasing levels of muscle sympathetic nerve activities (MSNA) resulted in a shift of the spectral power toward its LF component, whereas decreasing

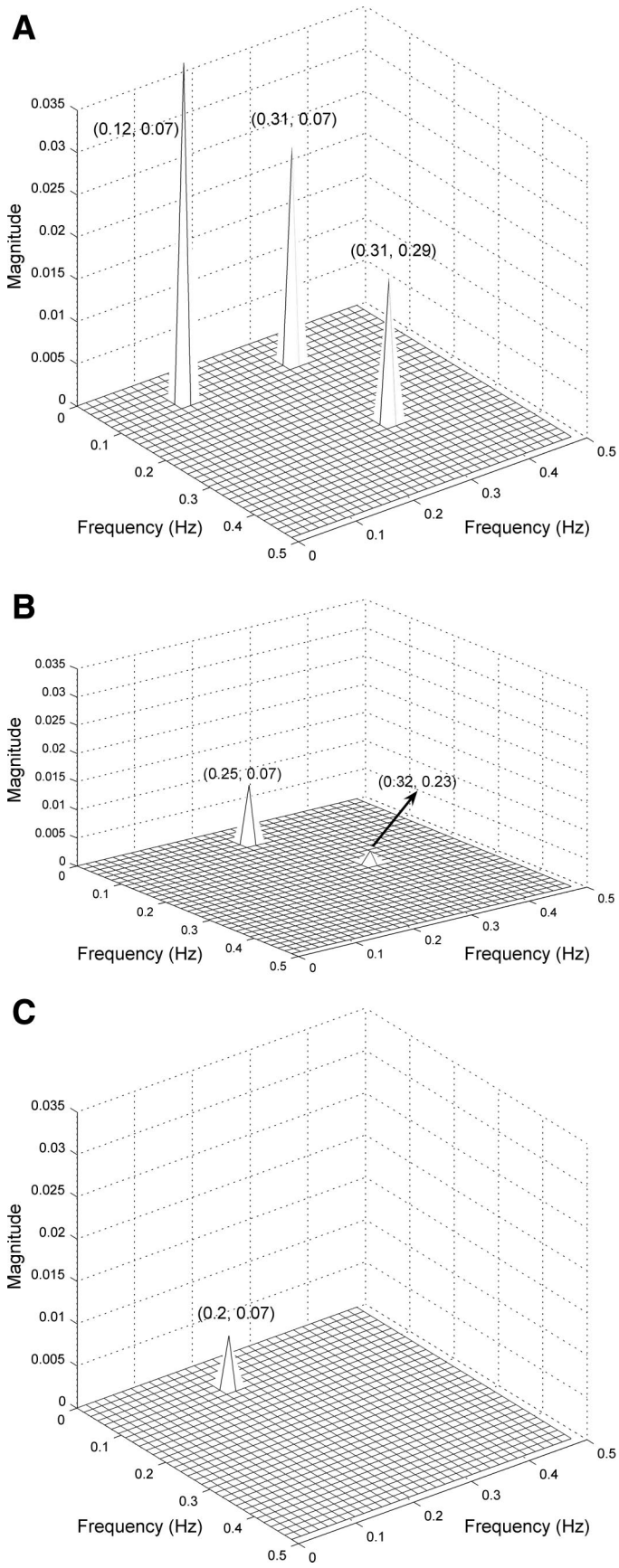

Fig. 3. Representative bispectrum results from a young healthy subject (*A*), old healthy subject (*B*), and acute myocardial infarction subject (*C*) in the supine position. The self-coupling peak in the young healthy subject disappears for both old healthy and acute myocardial infarction subjects.

Table 3. *Group average of bispectrum results indicating the presence of phase coupling for healthy young and old and AMI subjects during the supine position*

Supine	LF-HF	HF-HF
Young control	0.044±0.063	0.012±0.015
Old control	0.017±0.038	0.010±0.0021
AMI	0.0012±0.0026†	0.00061±0.00074*†

Values are means ± SD; $n = 16$ young control, 12 old control, and 35 acute myocardial infarction (AMI) subjects. *$P < 0.05$ between AMI and old control group; †$P < 0.05$ between AMI and young control group.

levels of MSNA were associated with a shift of MSNA spectral power toward the HF component (19). Thus the LF-LF coupling may indicate interactions between either the sympathetic system itself or the sympathetic and parasympathetic nervous systems. HF-HF most likely represents parasympathetic system self-coupling, given the fact that the presence of sympathetic nervous regulation is rather small in the HF bands (19); LF-HF may indicate either parasympathetic self-coupling or sympathetic and parasympathetic nervous system interactions. It is widely known that although the effect of parasympathetic regulation in the LF band is substantial (7, 23), its effect is not greater than the sympathetic system (1, 26a). Thus it is also plausible to consider LF-LF as the primarily coupling between the sympathetic system itself. Similarly, the LF-HF can be considered as primarily reflecting sympathetic and parasympathetic interactions. It should also be noted that an insufficient segment averaging of the bispectrum can lead to erroneous self-coupling peaks (e.g., HF-HF and LF-LF). In this scenario, even the surrogate data technique will not protect against false self-coupling peaks. Thus, when we observe self-coupled peaks, we do not have a good confidence whether the observed self-coupled peak is truly due to self coupling or artificially generated due to an insufficient number of bispectral segments (see *Eq. 3*). Given this limitation, the peaks in the LF-HF region are of primary interest and an interpretation of the peaks associated with either LF-LF or HF-HF will be limited in the discussion hereafter.

The evidence of nonlinear interactions between the sympathetic and parasympathetic nervous systems has been well documented in many experimental studies (12, 26, 26a). In one study, it was noted that decreased sympathetic nervous activity blunted the heart rate response to parasympathetic nervous system activation (15). Similarly, a decrease in MSNA was reported after the application of atropine (16). Quantitative analysis also found interactions between the two nervous systems. For example, using a combined wavelet and power spectral analysis, we found evidence of interactions between the sympathetic and parasympathetic nervous systems in the form of frequency modulation in the same young control subjects as used in this report (29). Interactions in the form of frequency modulation are also a consequence of the nonlinear properties of systems since nonlinear coupling can take many different forms. It has been suggested that in certain cases, the frequency modulation may produce quadratic terms, which in turn can lead to the presence of QPC (20). Thus, given these factors, it is not surprising that bispectral analysis provides evidence of the presence of nonlinear interactions in the same data. Furthermore, pharmacological interventions that are known to block either sympathetic or parasympathetic regulation confirmed the sensitivity of our approach. Indeed, we observed that phase coupling in all frequency bands was completely abolished by atropine alone or by both drugs, thereby lending credence to the observed interactions between the sympathetic and parasympathetic nervous activities in young healthy subjects for both body positions. It is interesting to note that atropine, which blocks parasympathetic activity, destroyed the presence of LF-HF nonlinear interactions in the young supine subjects. On the contrary, sympathetic blockade due to propranolol administration induced a trend of decrease in the magnitude of coupling compared with that of the control in the upright position, but it did not abolish the coupling. These findings can be interpreted as an indication of the important role played by the parasympathetic nervous system in the generation of QPC within HRV in physiological conditions. These results are in agreement with previous animal studies where the presence of the parasympathetic nervous activities in both the LF and HF bands was found (7, 23). This interpretation is further supported by the fact that during upright position, a condition that is known to induce spontaneously a sympathetic activation and a concurrent parasympathetic deactivation (14), the phase coupling was consistently reduced compared with that of the supine position. The involvement of the vagal component of the autonomic nervous system in producing nonlinear dynamics in the heart rate has also been demonstrated using nonlinear measures of complexity during conditions of altered parasympathetic activity (2–4, 21).

The importance of the parasympathetic modulation in originating sympathetic and parasympathetic nervous system nonlinear interactions was also confirmed in the post-MI patients. Indeed, we observed that the LF-HF coupling is essentially absent in AMI compared with young control subjects in both body positions, whereas nonsignificant coupling differences between young control and old control were found in both body positions. These results hold similarly for the HF-HF coupling, which was negligible in AMI patients compared with either young or the age-matched old control subjects. They agree with previous experimental evidence indicating that sympathetic neural activation is increased, whereas vagal activity is decreased in MI (8, 10). It has been suggested that one of the causes of the increased sympathetic activation and subsequent decreased vagal activity following AMI is related to the activation of cardiac sympathetic afferent fibers (13). Physiologically, the absence of coupling is an indication of the imbalance between the sympathetic and parasympathetic nervous systems. The imbalance between the cardiac parasympathetic and sympathetic nervous system is manifested as an

Table 4. *Group average of bispectrum results indicating the presence of phase coupling for healthy young and old and AMI subjects during the upright position*

Upright	LF-HF	HF-HF
Young control	0.026±0.031	0.0066±0.016
Old control	0.039±0.078	0.0037±0.0081
AMI	0.0011±0.0013*†	0.0016±0.0032

Values are means ± SD; $n = 22$ young control, 12 old control, and 35 AMI subjects. *$P < 0.05$ between AMI and old control group; †$P < 0.05$ between AMI and young control group.

absence of nonlinear coupling in the AMI subjects. The absence of nonlinear coupling in the cardiovascular dynamics after AMI was also found in a recent work by Nollo et al. (18). Using the same AMI heart rate data as presented in this study along with systolic arterial pressure (SAP) measured synchronously, they found decreased nonlinear coupling between the heart rate and SAP for the AMI subjects using a cross-conditional entropy method (18).

Potential Limitations

It should be noted that post-AMI patients enrolled in the study may not reflect a contemporary population in terms of revascularization procedure since the data were acquired during the GISSI-3 study.

In this study, the physiological interpretation of QPC between various frequency bands was based on the premise that these spectral dynamics represent interactions between the two branches of the autonomic nervous system. It should be recognized, however, that variations in heart rate dynamics may also arise due to complex interactions between several neural and nonneural mechanisms (15, 26a). For example, it was found that very LF (0.01–0.04 Hz) fluctuations in blood pressure depend on circulating catecholamines (22), whereas another study suggests the role of L-type Ca^{2+} channels (11).

Conclusion

The bispectrum, without the use of a surrogate data technique, has been hampered by its lack of specificity. Thus determining the presence of nonlinear coupling has been rather ad hoc. In addition, as shown in Fig. 1*A*, noise can lead to many erroneous bispectral peaks, thus creating difficulties in deciding which peaks are truly significant. These limitations were addressed by the use of a surrogate data technique, which has lead to statistically based decisions about the significance of coupling. Moreover, our technique was able to filter out any erroneous peaks that may have been generated due to noise contamination. Our results indicate that one possible discriminating dynamic for the AMI subjects is the absence of nonlinear interactions between the sympathetic and parasympathetic nervous systems, which is likely to reflect the depressed vagal regulation common to this disease. In both healthy young and old subjects, there were significant nonlinear interactions, but the magnitudes of coupling appear to decrease with older subjects in the supine position. Thus it can be summarized that autonomic imbalance progresses with age and becomes severe enough to entirely obliterate nonlinear interactions between the cardiac parasympathetic and sympathetic nervous systems in the AMI subjects. It is not clear at present whether the method will be sensitive enough to be used as a discriminator between normal subjects and people with slowly progressive cardiac diseases. Obtaining the data to answer this question will require a continuous monitoring of subjects pre- and post-AMI.

REFERENCES

1. **Akselrod S, Gordon D, Ubel FA, Shannon DC, Berger AC, Cohen RJ.** Power spectrum analysis of heart rate fluctuation: a quantitative probe of beat-to-beat cardiovascular control. *Science* 213: 220–222, 1981.
2. **Braun C, Kowallik P, Freking A, Hadeler D, Kniffki KD, Meesmann M.** Demonstration of nonlinear components in heart rate variability of healthy persons. *Am J Physiol Heart Circ Physiol* 275: H1577–H1584, 1998.
3. **Chon KH, Mullen TJ, Cohen RJ.** A dual-input nonlinear system analysis of autonomic modulation of heart rate. *IEEE Trans Biomed Eng* 43: 530–544, 1996.
4. **Fortrat JO, Yamamoto Y, Hughson RL.** Respiratory influences on non-linear dynamics of heart rate variability in humans. *Biol Cybern* 77: 1–10, 1997.
6. **Guzzetti S, Piccaluga E, Casati R, Cerutti S, Lombardi F, Pagani M, Malliani A.** Sympathetic predominance in essential hypertension: a study employing spectral analysis of heart rate variability. *J Hypertens* 6: 711–717, 1988.
7. **Houle MS, Billman GE.** Low-frequency component of the heart rate variability spectrum: a poor marker of sympathetic activity. *Am J Physiol Heart Circ Physiol* 276: H215–H223, 1999.
8. **Huikuri HV, Koistinen MJ, Yli-Mayry S, Airaksinen KE, Seppanen T, Ikaheimo MJ, Myerburg RJ.** Impaired low-frequency oscillations of heart rate in patients with prior acute myocardial infarction and life-threatening arrhythmias. *Am J Cardiol* 76: 56–60, 1995.
9. **Jose AD, Taylor RR.** Autonomic blockade by propranolol and atropine to study intrinsic myocardial function in man. *J Clin Invest* 48: 2019–2031, 1969.
10. **Kleiger RE, Miller JP, Bigger JT Jr, Moss AJ.** Decreased heart rate variability and its association with increased mortality after acute myocardial infarction. *Am J Cardiol* 59: 256–262, 1987.
11. **Langager AM, Hammerberg BE, Rotella DL, Stauss HM.** Very low-frequency blood pressure variability depends on voltage-gated L-type Ca^{2+} channels in conscious rats. *Am J Physiol Heart Circ Physiol* 292: H1321–H1327, 2007.
12. **Levy MN.** Sympathetic-parasympathetic interactions in the heart. *Circ Res* 29: 437–445, 1971.
13. **Malliani A, Montano N.** Emerging excitatory role of cardiovascular sympathetic afferents in pathophysiological conditions. *Hypertension* 39: 63–68, 2002.
14. **Malliani A, Pagani M, Lombardi F, Cerutti S.** Cardiovascular neural regulation explored in the frequency domain. *Circulation* 84: 482–492, 1991.
15. **Miyamoto T, Kawada T, Yanagiya Y, Inagaki M, Takaki H, Sugimachi M, Sunagawa K.** Cardiac sympathetic nerve stimulation does not attenuate dynamic vagal control of heart rate via α-adrenergic mechanism. *Am J Physiol Heart Circ Physiol* 287: H860–H865, 2004.
16. **Montano N, Cogliati C, Porta A, Pagani M, Malliani A, Narkiewicz K, Abboud FM, Birkett C, Somers VK.** Central vagotonic effects of atropine modulate spectral oscillations of sympathetic nerve activity. *Circulation* 98: 1394–1399, 1998.
17. **Nikias CL, Petropulu AP.** *Higher-Order Spectral Analysis: A Nonlinear Signal Processing Framework*. Englewood Cliffs, NJ: Prentice Hall, 1993.
18. **Nollo G, Faes L, Porta A, Pellegrini B, Ravelli F, Del Greco M, Disertori M, Antolini R.** Evidence of unbalanced regulatory mechanism of heart rate and systolic pressure after acute myocardial infarction. *Am J Physiol Heart Circ Physiol* 283: H1200–H1207, 2002.
19. **Pagani M, Montano N, Porta A, Malliani A, Abboud FM, Birkett C, Somers VK.** Relationship between spectral components of cardiovascular variabilities and direct measures of muscle sympathetic nerve activity in humans. *Circulation* 95: 1441–1448, 1997.
20. **Patwardhan A, Wang K, Moghe S, Leonelli F.** Bispectral energies within electrocardiograms during ventricular fibrillation are correlated with defibrillation shock outcome. *Ann Biomed Eng* 27: 171–179, 1999.
21. **Porta A, Baselli G, Guzzetti S, Pagani M, Malliani A, Cerutti S.** Prediction of short cardiovascular variability signals based on conditional distribution. *IEEE Trans Biomed Eng* 47: 1555–1564, 2000.
22. **Radaelli A, Castiglioni P, Centola M, Cesana F, Balestri G, Ferrari AU, Di Rienzo M.** Adrenergic origin of very low-frequency blood pressure oscillations in the unanesthetized rat. *Am J Physiol Heart Circ Physiol* 290: H357–H364, 2006.
23. **Randall DC, Brown DR, Raisch RM, Yingling JD, Randall WC.** SA nodal parasympathectomy delineates autonomic control of heart rate power spectrum. *Am J Physiol Heart Circ Physiol* 260: H985–H988, 1991.
24. **Schreiber T, Schmitz A.** Surrogate time series. *Physica D* 142: 346–382, 2000.
25. **Siu K, Ahn JM, Ju K, Lee M, Shin K, Chon KH.** Statistical approach to quantify the presence of phase coupling using the bispectrum. *IEEE Trans Biomed Eng* 55: 1512–1520, 2008.
26. **Sunagawa K, Kawada T, Nakahara T.** Dynamic nonlinear vago-sympathetic interaction in regulating heart rate. *Heart Vessels* 13: 157–174, 1998.

26a. **Task Force of the European Society of Cardiology and the North American Society of Pacing and Electrophysiology Circulation.** Heart

rate variability: standards of measurement, physiological interpretation, and clinical use. *Eur Heart J* 93: 1043–1065, 1996.

27. **Theiler J, Eubank S, Longtin A, Galdrikian B, Farmer JD.** Testing for nonlinearity in time series: the method of surrogate data. In: *Interpretation of Time Series from Nonlinear Mechanical Systems*. Warwick, United Kindom, 1992, p. 77–94.
28. **Zar JH.** *Biostatistical Analysis* (4th ed.). Upper Saddle River, NJ: Prentice Hall, 1999.
29. **Zhong Y, Bai Y, Yang B, Ju K, Shin K, Lee M, Jan KM, Chon KH.** Autonomic nervous nonlinear interactions lead to frequency modulation between low- and high-frequency bands of the heart rate variability spectrum. *Am J Physiol Regul Integr Comp Physiol* 293: R1961–R1968, 2007.